cells

MDPI

Article

Stefin B and Cystatin C Deficiency Suppresses Tumor Growth and Alters Tumor Microenvironment in a Breast Cancer Model

Petra Matjan Štefin [1,2], Janja Završnik [1], Miha Butinar [1], Georgy Mikhaylov [1,*], Boris Turk [1,3] and Olga Vasiljeva [1,*]

[1] Department of Biochemistry and Molecular and Structural Biology, Jožef Stefan Institute, 1000 Ljubljana, Slovenia; petra.matjan-stefin@ijs.si (P.M.Š.); janja.zavrsnik@gmail.com (J.Z.); boris.turk@ijs.si (B.T.)
[2] Jožef Stefan International Postgraduate School, 1000 Ljubljana, Slovenia
[3] Faculty of Chemistry and Chemical Technology, University of Ljubljana, 1000 Ljubljana, Slovenia
* Correspondence: georgy.mikhaylov@ijs.si (G.M.); olga.vasiljeva@ijs.si (O.V.)

Highlights

What are the main findings?

- Combined deficiency of stefin B and cystatin C in the PyMT breast cancer mouse model significantly delays tumor onset, suppresses primary tumor growth, and reduces the incidence of lung metastases compared with wild-type controls.
- Increased intratumoral infiltration of M1-polarized macrophages is proposed to disrupt tumor-associated immunosuppressive mechanisms, thereby impairing tumor cell survival and proliferation.

What are the implications of the main findings?

- Simultaneous ablation of both cysteine cathepsins inhibitors uncovers therapeutic vulnerabilities that are not apparent with single-target inhibition, highlighting the potential advantage of dual-targeting strategies.
- These results redefine the functional paradigm of cystatin family inhibitors in breast cancer, demonstrating a context-dependent tumor-promoting role rather than a uniformly protective function.

Abstract

Background/Objectives: Cysteine cathepsins and their endogenous inhibitors have been shown to possess context-dependent functions in cancer progression, including the regulation of tumor metabolic pathways. Stefin B and cystatin C, intracellular and extracellular protease inhibitors, respectively, can modulate tumor biology through protease-dependent and protease-independent mechanisms. This study investigated their combined functions and potential roles as tumor promoters in breast cancer in a spontaneous breast cancer mouse model (PyMT mice). **Methods**: We generated PyMT transgenic mice lacking both stefin B and cystatin C (double-knockout, DKO) and compared their tumor growth kinetics, proliferation, apoptosis, and metastatic burden with those of wild-type control mice. Immunohistochemistry was performed to characterize tumor macrophage infiltration and polarization. **Results**: DKO mice demonstrated delayed tumor onset, significantly slower tumor growth, reduced proliferation, increased apoptosis, and fewer lung metastases compared to wild-type controls. Immunohistochemistry revealed enhanced macrophage infiltration of the tumors, accompanied by a pronounced shift toward antitumorigenic M1 ($CD86^+$) polarization, while M2 ($CD206^+$) populations remained unchanged, indicating an immunological reprogramming of the tumor microenvironment toward a pro-inflammatory, tumor-suppressive state. **Conclusions**: Our results demonstrated a potential function of

Check for updates

Academic Editors: Arnaud Blomme and Cyril Corbet

Received: 10 January 2026
Revised: 7 February 2026
Accepted: 12 February 2026
Published: 17 February 2026

Copyright: © 2026 by the authors. Licensee MDPI, Basel, Switzerland. This article is an open access article distributed under the terms and conditions of the Creative Commons Attribution (CC BY) license.

stefin B and cystatin C as tumor promoters in breast cancer through complementary mechanisms. Simultaneous depletion of both inhibitors revealed synergistic effects and remodeled the immune microenvironment to favor tumor suppression. These results suggest previously unknown roles for stefin B and cystatin C in tumor development and progression, which encourage further investigation of the cancer metabolic mechanisms underlying tumor behavior and their dynamic interplay with the microenvironment.

Keywords: cancer metabolism; cysteine cathepsins; protease inhibitors; breast cancer; tumor microenvironment; macrophage polarization

1. Introduction

Cysteine cathepsins are lysosomal cysteine proteases that belong to a group of proteolytic enzymes involved in regulating numerous normal biological processes, including key metabolic pathways. In recent years, their broader function has been discovered not only in the endolysosomal compartment but also in the cytoplasm, the cell nucleus, and the extracellular milieu, which indicates their extensive biological impact [1–3]. Cysteine cathepsins are involved in fundamental cellular processes, including protein degradation, protein and lipid metabolism, autophagy, growth factor receptor recycling, and cellular stress signaling, as well as in broader physiological functions such as tissue homeostasis, apoptosis, lysosome-mediated cell death, immune responses, and development and differentiation, all of which are tightly linked to cellular metabolism and tumor metabolic plasticity [1,4,5]. Despite their critical roles in multiple physiological conditions, lysosomal cathepsins have been implicated in various pathologies, including neurodegeneration, cardiovascular diseases, bone disorders, autoimmune disorders, and cancer [3,6–8].

In many cancer types, increased expression and activity of lysosomal cathepsins have been associated with disease progression and a poor prognosis [9–13]. Increased proteolytic activity of cysteine cathepsins contributes to tumor progression through multiple interconnected mechanisms, including activation and processing of growth factors, cytokines, and chemokines in the tumor microenvironment, as well as the degradation and reorganization of extracellular matrix, leading to cancer spread and tumor-promoting inflammation [4,8,12,14,15]. Furthermore, these enzymes modulate the immune response by influencing the recruitment and function of immune cells, including antigen presentation and cytokine processing, often resulting in immune evasion and suppression within the tumor microenvironment [16]. Cysteine cathepsins can also influence extracellular and intracellular signaling pathways by processing cytokines, growth factors, and adhesion molecules, thereby modulating key pathways such as TNF-α/MAPK (tumor necrosis factor-alpha/mitogen-activated protein kinase) [17], TGF-β1 (transforming growth factor-beta 1) [18], and PI3K (phosphoinositide 3-kinase) signaling [19], which regulate tumor proliferation, survival, and migration. Additionally, proteases are known to operate within a complex protease network termed the »protease web« [20], thereby interacting with many other proteases and their inhibitors to initiate cascades that could contribute to tumor growth, angiogenesis, immune modulation, and metastasis [15,21].

The proteolytic activity of cysteine cathepsins is regulated by various mechanisms, the predominant ones being zymogen activation and inhibition by endogenous inhibitors [22]. Among cysteine cathepsin inhibitors, the cystatin superfamily is the most broadly known and is classified into three major families: stefins (family I), cystatins (family II), and kininogens (family III). Stefin A and B (cystatin A and B) are the main types of stefins that belong to family I and have a molecular mass of ~11 kDa. These inhibitors are

unglycosylated, lack a signal sequence, contain disulfide bonds, and are localized in the cytosol, mitochondria, and nucleus [23]. They reversibly inhibit cathepsin B, H, S, and L, thereby protecting the cell from lysosomal enzyme leakage [24]. Under physiological conditions, stefin B acts as an intracellular inhibitor that protects cells from cathepsins leaking from lysosomes and helps limit oxidative stress by reducing mitochondrial damage and ROS (reactive oxygen species) production [23,25]. Stefin B also influences autophagy via AMPK/mTOR (AMP-activated protein kinase/mechanistic target of rapamycin) pathways, has chaperone-like functions by binding proteins like amyloid-β, and modulates inflammasome activation and immune responses [23,26]. In contrast to the more restricted expression of stefin A, stefin B is widely distributed in various cell types and tissues [27]. Studies across human cancers reveal contradictory roles for stefin B, functioning as either a tumor suppressor or promoter depending on cancer type and context [28–34]. Stefin B shows protective effects against oxidative stress and apoptosis in breast cancer models [35], but its high expression is linked to advanced stages and metastasis in hepatocellular carcinoma and to poorer survival in colorectal cancer [31,36]. Notably, in advanced cancer stages and metastasis, decreased levels of stefin B correlate with tumor progression [37,38]. These contradictory observations point to diverse functions of stefin B during cancer progression and metastasis, and thus call for further exploration of its role in multifaceted disease conditions using experimental models and biological samples.

The family of cystatins includes cystatin C, D, E/M, S, SA, and SN, with molecular masses in the range of 13–14 kDa. The members of family II are extracellular inhibitors, have disulfide bonds at the carboxy terminus of the molecule, and some are glycosylated. Contrary to stefins, cystatins have a signal sequence that allows transmembrane secretion, representing an essential regulatory mechanism for the extracellular activity of cysteine cathepsins. In family II, cystatin C is recognized as the most essential and potent extracellular inhibitor of cathepsins [1]. Specifically, it inhibits cathepsins L and S at picomolar concentrations and cathepsins B, H, and C at nanomolar concentrations [39]. Cystatin C is produced by all nucleated cells and primarily acts as an extracellular cysteine protease inhibitor [40]. Beyond protease inhibition, it also exhibits neuroprotective effects by inducing autophagy, promoting neurogenesis, and inhibiting amyloid-β aggregation [41,42]. It also contributes to cardiovascular homeostasis by regulating elastolytic proteases and modulating immune processes such as antigen presentation and cytokine processing [43]. Structurally, cystatin C is a non-glycosylated protein (~13.3 kDa) [44,45], and it has been associated with various pathologies, including cancer.

Many reports show its expression in tumor tissues; however, its specific role in tumor progression remains unclear [40]. Similar to stefin B, numerous studies show opposing effects of cystatin C on tumor growth and metastasis, in which it acts either as a promoter or a suppressor [44,46,47]. Cystatin C plays context-dependent roles that vary across tumor types and disease stages. Its expression is decreased in skin cancer, increased in ovarian cancer, and inversely correlated with tumor grade in glioma [4,44,48,49]. Multiple studies have been conducted to investigate the role of cystatin C using pre-clinical in vivo models. In the PyMT breast cancer model, cystatin C knockout resulted in decreased tumor growth and reduced cell proliferation, suggesting its involvement in proliferation signaling beyond protease inhibition [48]. Similarly, CRISPR-mediated cystatin C knockout in a syngeneic pancreatic cancer mouse model significantly reduced tumor growth and diminished recruitment of immunosuppressive TREM2+ (triggering receptor expressed on myeloid cells 2) macrophages, supporting cystatin C's role in tumor promotion and immune microenvironment remodeling [50]. Additionally, an in vitro study using primary macrophages isolated from cystatin C-deficient mice has demonstrated that cystatin C affects macrophage polarization and local cytokine profiles, thereby modulating the balance between anti-tumor

immunity and immunosuppression within the tumor microenvironment [51]. While its inhibitory activity against cathepsins may partly explain these contrasting effects on cancer progression, some evidence suggests that cathepsin-inhibition-independent mechanisms, such as disruption of TGF-β signaling and modulation of epithelial–mesenchymal transition (EMT), also contribute to cystatin C's complex impact on tumor growth and metastasis [46,47].

While individual roles of stefin B and cystatin C in cancer have been studied, their combined impact on breast cancer progression remains unexplored. Our previous studies revealed distinct roles for stefin B and cystatin C in breast cancer progression. Stefin B deficiency resulted in reduced tumor burden through increased tumor cell death and enhanced sensitivity to oxidative and lysosomal stress-induced apoptosis, without affecting proliferation or metastasis [35]. In contrast, cystatin C deficiency reduced tumor growth through decreased tumor cell proliferation and increased extracellular cathepsin activity, with minimal effects on apoptosis [48]. These findings demonstrated that stefin B primarily modulates tumor cell survival under stress, whereas cystatin C controls proliferative signaling in the extracellular tumor microenvironment. To investigate their combined effect on tumor progression and dissemination, we generated a stefin B and cystatin C double-knockout mouse cancer model by crossing stefin B and cystatin C double-knockout mice with Polyoma Middle T antigen (PyMT) mice, a strain susceptible to mammary tumor development. The results show that the simultaneous absence of stefin B and cystatin C led to slower tumor growth and reduced metastasis compared with control mice, suggesting that these proteins can promote breast cancer by supporting metabolic plasticity in tumor cells, independently of their cysteine cathepsin-inhibitory function.

2. Materials and Methods

2.1. Animals

Mice were used in accordance with the Administration of the Republic of Slovenia for Food Safety, Veterinary, and Plant Protection (ethical approval codes: U34401-35/2014/2, U34401-6/2019/5, and U34401-5/2022/15). Procedures for animal care and experiments were in accordance with the "Guide for the Care and Use in Laboratory Animals".

An FVB/N transgenic mouse strain expressing PyMT under the control of the MMTV long-terminal repeat promoter (FVB/N-TgN (MMTVPyVT)634-Mul) was kindly provided by Thomas Reinheckel (Institut für Molekulare Medizin und Zellforschung, Albert-Ludvig Universitat, Freiburg, Germany), and the mice were maintained in our animal facility. The cystatin C knockout ($CstC^{-/-}$) mice of the C57BL/6 strain were kindly provided by Dr. Anders Grubb (Lund University, Lund, Sweden). $CstC^{-/-}$ mice were backcrossed for more than 10 generations to the FVB/N transgenic mouse strain expressing PyMT under the control of the MMTV long-terminal repeat promoter (FVB/N-TgN (MMTVPyVT)634-Mul). The StfB-deficient ($StfB^{-/-}$) mouse strain was kindly provided by Dr Richard M. Myers. $StfB^{-/-}$ mice were backcrossed for eight generations to the transgenic mouse strain expressing PyMT under the control of MMTV long-terminal repeat promoter (FVB/N-TgN (MMTVPyVT)634-Mul). Stefin B and cystatin C double-knockout PyMT mice were generated by crossing $StfB^{+/-}CstC^{+/-}$ female and $PyMT;StfB^{+/-}CstC^{+/-}$ male mice. $PyMT;StfB^{-/-}CstC^{+/-}$ and $PyMT;StfB^{+/-}CstC^{-/-}$ males were also used. Offspring with various combinations of these genes were produced, and those completely lacking both stefin B and cystatin C, in addition to carrying the PyMT gene, were selected and designated as PyMT;DKO. Maintenance and breeding of the animals used in this study were performed in accordance with Slovene law for animal protection.

Animals were bred and housed in the Laboratory for Experimental Animals at the Jožef Stefan Institute, a facility designed for the maintenance of laboratory rodents. Housing

conditions included climate control with constant temperature maintained between 20–24 °C and relative humidity between 50–65%. Mice were housed in standard-sized cages (Tecniplast 1264C Eurostandard Type II, Tecniplast, West Chester, PA, USA) at a density of up to 5 animals per cage. Cages were labeled according to institutional protocols. Individual mice were identified with ear tags to facilitate individual monitoring. Animals had ad libitum access to water and standard laboratory diet. Sterilized bedding material was used to maintain hygienic housing conditions.

2.2. Tumor Progression Study

Group sizes were based on animal availability and the 3R principle (Reduction). All phenotypically normal female mice with the appropriate genotypes were included; no animals or data points were excluded.

Beginning at 30 days of age, female mice were palpated three times weekly in a genotype-blinded manner to monitor the onset of mammary tumors. Thirty days following the appearance of the first tumor, tumor diameters were measured using a digital caliper. At 14 weeks of age, the mice were euthanized, and all ten tumors from each animal were carefully excised, measured, and weighed.

2.3. Histomorphometry

For volumetric measurement of total lung metastasis or disseminated tumor colonies in the lungs, paraffin-embedded lungs were sectioned at 5 µm thickness from at least three distinct planes. Each section was subsequently stained with hematoxylin and eosin. The average size of metastases was quantified using computer-assisted analysis with CellSens Imaging software (Version 1.17; Olympus, Tokyo, Japan).

2.4. Immunohistochemistry

Left thoracic tumors of PyMT;WT and PyMT;DKO mice were collected and fixed in 10% neutral-buffered formalin overnight and then processed for paraffin embedding. Formalin-fixed, paraffin-embedded samples of tumors were sectioned into 5 µm thick slices and affixed to glass slides. The slides were deparaffinized and rehydrated through graded alcohols to distilled water, followed by antigen retrieval with citrate buffer, pH 6.0, and, for macrophage detection, with Proteinase K (20 µg/mL in TE buffer, pH 8.0). Endogenous peroxidase was quenched with 0.3% hydrogen peroxide. The sections were stained with antibodies against Ki67 (Dako, Carpinteria, CA, USA; M724901, rabbit monoclonal, dilution 1:50), F4/80 (Novus Biologicals, Centennial, CO, USA; NB600-404, rat monoclonal, dilution 1:100), CD86 (Cell Signaling technology, Danvers, MA, USA; 19589S, rabbit monoclonal, dilution 1:200), and CD206 (Cell Signaling technology, Danvers, MA, USA; 24595, rabbit monoclonal, dilution 1:500). A TUNEL assay (ApopTag; Oncor) was used for the in situ measurement of DNA fragmentation of dying cells. Detection of primary antibodies was performed using the Vectastain Elite ABC kit (Vector Laboratories, Inc., Burlingame, CA, USA) according to the manufacturer's instructions, and staining was visualized with DAB (Sigma–Aldrich, Steinheim, Germany). The slides were counterstained with hematoxylin and imaged using an IX81 bright-field microscope (Olympus, Tokyo, Japan) and Olympus CellSens Imaging software (Version 1.17). Tissue sections of each tumor were histologically examined for the proliferation marker Ki67, cell death (TUNEL staining), and the macrophage markers F4/80, CD86, and CD206, as described [52]. For Ki67, TUNEL, F4/80, CD86, and CD206 data assessment, 10 fields per tumor were randomly selected at 60× and quantified using ImageJ (Version 1.54p). Histological evaluation and quantification were performed in a blinded manner with respect to genotype.

2.5. Isolation of Primary Tumor Cells from PyMT-Induced Mammary Carcinomas

Primary PyMT tumor cells were isolated and cultured according to previously published methods [53].

2.6. DNA Replication Analysis by BrdU Incorporation

The BrdU Cell Proliferation Kit was obtained from EMD Millipore Corporation (Billerica, MA, USA). Primary tumor cells were seeded in 96-well plates at a density of 1×10^5 cells/mL and incubated with bromodeoxyuridine (BrdU) for 4 h. BrdU incorporation was then measured following the manufacturer's protocol using a Tecan Safire microplate reader (Tecan, Gröding, Austria) at 450 nm, with absorbance at 540 nm subtracted.

2.7. Assessment of Cathepsin Enzyme Activity

Cathepsin activity was assessed through the hydrolysis of the fluorogenic substrate Z-Phe-Arg-4-methyl-coumarin-7-amide (Z-Phe-Arg-AMC; Bachem, Bubendorf, Switzerland). Primary tumors were homogenized in lysis buffer (250 mM TRIS, 10 mM EDTA, 0.1% Triton X-100, pH 6.8) using an Ultraturrax (IKA, Staufen, Germany). For cell lysates, tumor cells were incubated in RIPA lysis buffer. A total of 20 µg of each sample was combined in a 96-well plate with 0.1 M phosphate buffer (1 mM EDTA, 0.1% v/v PEG, 1 mM DTT, pH 6), either in the presence or absence of 10 µM cysteine cathepsin inhibitor E64. After a 15 min incubation at 37 °C, Z-Phe-Arg-AMC was added to a final concentration of 30 µM, and substrate hydrolysis was monitored continuously for 15 min using a Tecan Safire microplate reader (Tecan, Gröding, Austria) at excitation and emission wavelengths of 370 nm and 460 nm, respectively.

For measurements in conditioned media, PyMT primary tumor cells of both genotypes were seeded in 12-well plates at 7.5×10^5 cells per well and incubated for 2 h at 37 °C in PBS (Lonza, Verviers, Belgium). Following incubation, 50 µL of PBS from each well was transferred to a 96-well plate containing 0.1 M phosphate buffer, and the assay was carried out as described above.

2.8. Immunoblotting

Tumor and mammary gland tissues were homogenized, and protein extracts with normalized concentrations were resolved SDS–PAGE using 12.5% gels and transferred onto polyvinylidene difluoride (PVDF) membranes. Membranes were probed with anti-CstC antibody (Abcam, Cambridge, UK; ab109508, 1:100,000) and anti-StfB antibody (R&D Systems, Minneapolis, MN, USA; MAB1409, 1:5000). Anti-β-actin (Sigma-Aldrich, St. Louis, MO, USA; A1978, mouse monoclonal, 1:5000) was used as a loading control. Appropriate secondary antibodies were applied at a 1:5000 dilution.

2.9. Statistical Analysis

Quantitative data are presented as the means ± SEs. The differences were compared using Student's *t*-test. Proportions were compared using the Chi-square test. *p*-values less than 0.05 were considered statistically significant.

Power analysis for the primary endpoint (cumulative tumor weight) was conducted using G*Power 3.1 to assess study robustness.

3. Results

3.1. Generation and Characterization of PyMT Transgenic Mice with Combined Stefin B and Cystatin C Deficiency

To explore the impact of combined deficiency of stefin B (StfB) and cystatin C (CstC) on tumor progression, we established double-knockout $StfB^{-/-}$;$CstC^{-/-}$ (DKO) mice. These

mice exhibited no apparent phenotypic abnormalities at 14 weeks of age. They were then crossed with FVB/N-Tg (MMTV-PyVT)634Mul/J transgenic mice (commonly referred to as FVB/PyMT), a widely utilized model of spontaneous mammary tumorigenesis. In this murine model, the polyoma virus middle T antigen (PyMT) is expressed under the control of the mouse mammary tumor virus (MMTV) promoter, resulting in the rapid onset of multifocal mammary tumors that undergo various stages of progression, including hyperplasia, adenoma, and invasive carcinoma, ultimately leading to spontaneous pulmonary metastases. The FVB/PyMT model closely mirrors key aspects of human breast cancer, making it highly suitable for studying tumor development, immune interactions, and therapeutic responses [54,55]. For further investigation, two groups of female mice hemizygous for the PyMT transgene were generated: PyMT;WT (wild-type) and PyMT;DKO (double-knockout). Histological examination of tissues from both groups did not reveal any major morphological abnormalities or deviations (Figure S1).

Depletion of StfB and CstC in PyMT tumors was confirmed by Western blot analysis of mammary tumor tissues from 14-week-old PyMT;WT, PyMT;*StfB*$^{-/-}$, PyMT;*CstC*$^{-/-}$, and PyMT;DKO mice. While the presence of both inhibitors was confirmed in wild-type tumors (PyMT;WT), their expression was absent in the respective knockout groups. Tumors from double-knockout mice (PyMT;DKO) showed a complete loss of both inhibitors (Figure 1A,B), supporting the use of this model for further investigations into their roles in breast cancer development.

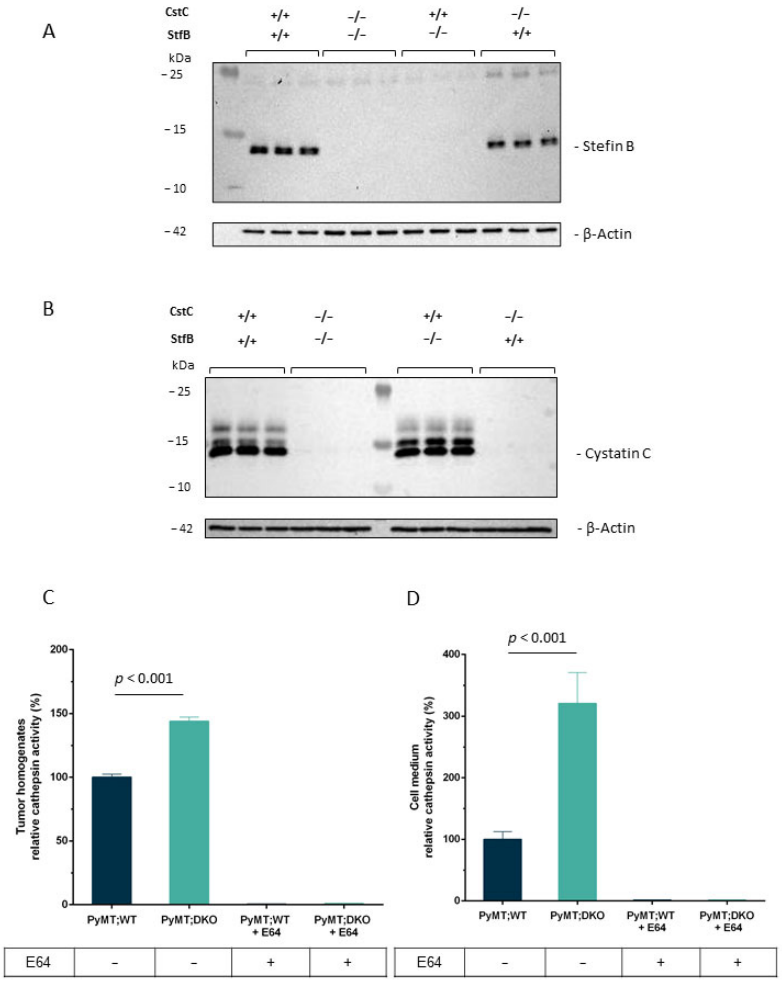

Figure 1. Expression of stefin B and cystatin C, and cysteine cathepsin activity, in PyMT mammary tumors of different genotypes. (**A**) Western blot for stefin B (StfB) in mammary tumors from wild-type

(PyMT;WT; n = 3), stefin B knockout (PyMT;*StfB*$^{-/-}$; n = 3), cystatin C knockout (PyMT;*CstC*$^{-/-}$; n = 3), and double-knockout (PyMT;DKO; n = 3) mice at 14 weeks of age. StfB is absent in PyMT;*StfB*$^{-/-}$ and PyMT;DKO tumors, confirming successful knockout. β-actin was used as a loading control. (**B**) Western blot for cystatin C (CstC) in the same tumor samples. CstC is absent in PyMT;*CstC*$^{-/-}$ and PyMT;DKO tumors, verifying successful knockout. β-actin was used as a loading control. (**C**) Relative cathepsin activity determined in homogenates of PyMT tumors (PyMT;WT, n = 4; PyMT;DKO, n = 3). Data represent biological replicates from independent tumors derived from different mice. Activity was measured as Z-Phe-Arg-AMC hydrolysis in the presence or absence of E64. Differences were analyzed using Student's *t*-test. (**D**) Relative cathepsin activity determined in cell culture medium of primary tumor cells (PyMT;WT, n = 3; PyMT;DKO, n = 3). Data represent biological replicates from independent primary tumor cell isolates derived from different mice. Activity was measured as Z-Phe-Arg-AMC hydrolysis in the presence or absence of E64. Differences between groups were analyzed using Student's *t*-test.

3.2. Impact of Stefin B and Cystatin C Depletion on Protease Activity in PyMT Mammary Tumors

To assess the impact of stefin B and cystatin C deletion on cysteine cathepsin activity in PyMT tumors, we analyzed tumor homogenates and conditioned media of primary PyMT;DKO and PyMT;WT tumor cells with the fluorogenic substrate Z-Phe-Arg-AMC, cleaved by most cysteine cathepsins. A significant increase in substrate cleavage in the PyMT;DKO group compared to the PyMT;WT group was detected, suggesting the role of both inhibitors in the regulation of protease activity in the PyMT model (Figure 1C,D). Notably, a ~3-fold increase in protease activity was detected in the conditioned media of the PyMT;DKO group (Figure 1D), indicating the importance of the extracellular protease inhibitor in restraining the activity of secreted cysteine cathepsins. The addition of E64, a broad-spectrum inhibitor of cysteine cathepsins, confirmed that the measured protease activity was attributable to cysteine cathepsins.

3.3. Progression and Metastasis of Stefin B and Cystatin C-Depleted PyMT-Induced Mammary Tumors

The development of mammary tumors in both experimental groups was assessed starting on day 30 after birth. PyMT;DKO mice showed a slight delay in tumor onset compared to PyMT;WT controls, with median onset at day 38 versus day 36, respectively. Kaplan–Meier analysis of tumor onset using a log-rank test revealed a significant delay in tumor development in the PyMT;DKO mice group ($p < 0.05$) (Figure 2A).

To compare tumor growth and progression between the groups, the volumes of the first two palpable mammary tumors were measured 30 days after the first tumor detection and grouped according to their diameter into three categories: small (<5 mm), medium (5–10 mm), and large (>10 mm). Compared to PyMT;WT, mammary tumors from PyMT;DKO mice were significantly smaller (Figure 2B), suggesting that ablation of both cystatins impairs tumor progression in the PyMT mammary cancer model. The reduced tumor size was further substantiated by ex vivo analysis, in which the collective weight of all 10 mammary tumors from 14-week-old mice was quantified. The average weight of tumors from PyMT;DKO mice was 5.8 g, which is 41% lower compared to tumors from PyMT;WT mice, which had an average tumor weight of 9.8 g (Figure 2C). These findings thus suggest that simultaneous deletion of CstC and StfB reduces tumor burden (cumulative tumor weight) in the PyMT mammary cancer model.

We next investigated the impact of CstC and StfB depletion on metastatic progression. In the MMTV;PyMT mouse model, lung metastases typically develop by 14 weeks of age in most animals. Therefore, we used computer-assisted histomorphometry to analyze the number and cumulative size of pulmonary metastases in sequential lung tissue sections from both experimental groups at 14 weeks of age. The analysis showed that the PyMT;DKO mice had a significantly lower number of lung metastases per unit area of lung tissue

compared to the PyMT;WT group (0.26/mm^2 in the PyMT;WT group, 0.05/mm^2 in the PyMT;DKO group) (Figure 2D). However, there was no statistically significant difference in the average size of the lung metastases between the two groups (Figure 2E). Our data thus indicate that the lack of stefin B and cystatin C expression may reduce metastatic seeding or early colonization of PyMT tumor cells, thus resulting in fewer metastatic lesions, while having no significant effect on the growth of metastases once established, as evidenced by comparable lesion size between groups.

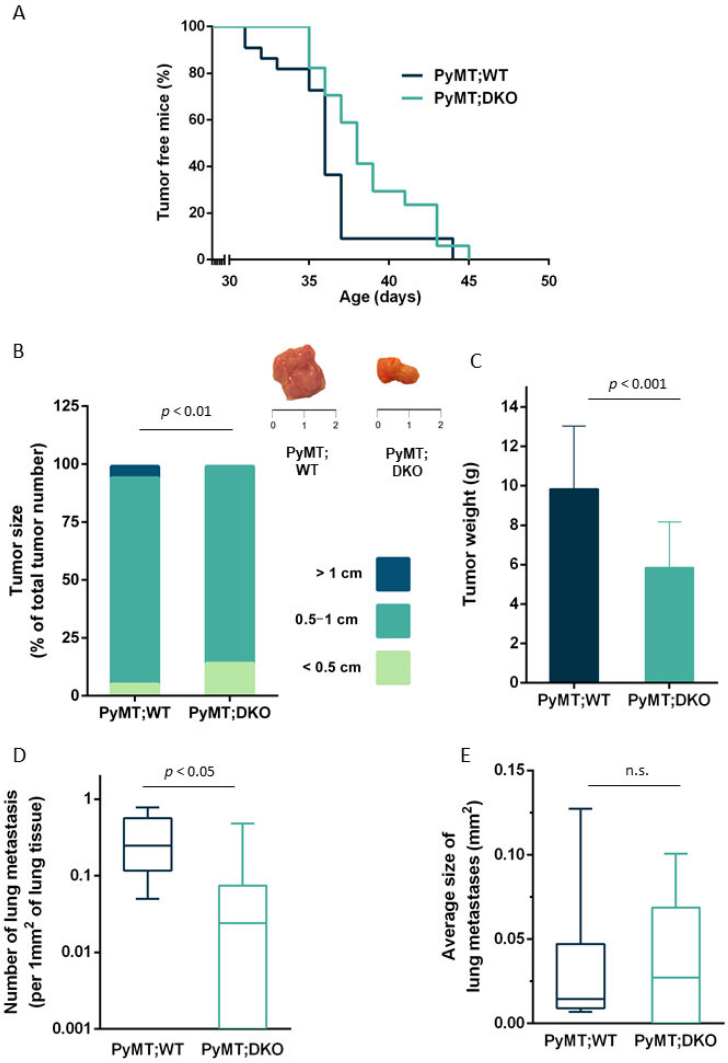

Figure 2. Effect of stefin B and cystatin C deficiency on tumor growth and metastasis in PyMT-induced mammary tumors. (**A**) Kaplan–Meier survival curves comparing tumor-free survival in PyMT;WT mice (n = 22; black line) and PyMT;DKO mice (n = 17; gray line). Statistical analysis using the log-rank test indicates a significant difference in tumor-free survival between the two groups ($p < 0.05$), with the PyMT;DKO group showing a delayed onset of tumors and longer survival than PyMT;WT mice. The hazard ratio (HR) for PyMT;DKO versus PyMT;WT group was 0.59 (95% CI: 0.24–0.85). Differences were analyzed using the log-rank test. (**B**) Size of 2 individual mammary tumors 30 days after the first detection in PyMT;WT (n = 37) and PyMT;DKO (n = 34) mouse cohorts. $p < 0.01$ by the chi-square test. Representative images show excised mammary tumors from PyMT;WT, and PyMT;DKO mice at 14 weeks of age. (**C**) The cumulative tumor weight per mouse for all mammary tumors was calculated for PyMT;WT (n = 13) and PyMT;DKO (n = 12) mice at 14 weeks of age. Differences were analyzed using Student's *t*-test, $p < 0.001$. Histomorphometric analysis of the number (**D**) and average size (**E**) of lung metastasis in PyMT;WT (n = 14) and PyMT;DKO (n = 14) female mice at 14 weeks. n.s., not significant. The number of metastases was calculated per 1 mm^2 of lung tissue. Differences were analyzed using Student's *t*-test.

3.4. Impact of Stefin B and Cystatin C Deficiency on Tumor Cell Proliferation and Cell Death

We further analyzed the effects of stefin B and cystatin C deficiency on the fundamental biological processes underlying tumor progression, including cell proliferation and cell death, within late-stage primary PyMT tumors. Immunohistochemical evaluation of the proliferation marker Ki67 was employed to assess cell proliferation in PyMT tumors derived from PyMT;WT and PyMT;DKO mice. Our findings indicate a significant reduction in the Ki67 proliferation index in PyMT;DKO tumors (6.6%) compared to PyMT;WT tumors (24%) (Figure 3A), consistent with the reduced size of PyMT;DKO tumors. Furthermore, supporting the Ki67 immunohistochemistry data obtained from tumor tissue, significantly lower proliferation of primary tumor cells isolated from PyMT;DKO tumors was detected in vitro using a BrdU (5-bromo-2′-deoxyuridine) assay, which quantifies cell proliferation by detecting BrdU incorporated into newly synthesized DNA (Figure S2).

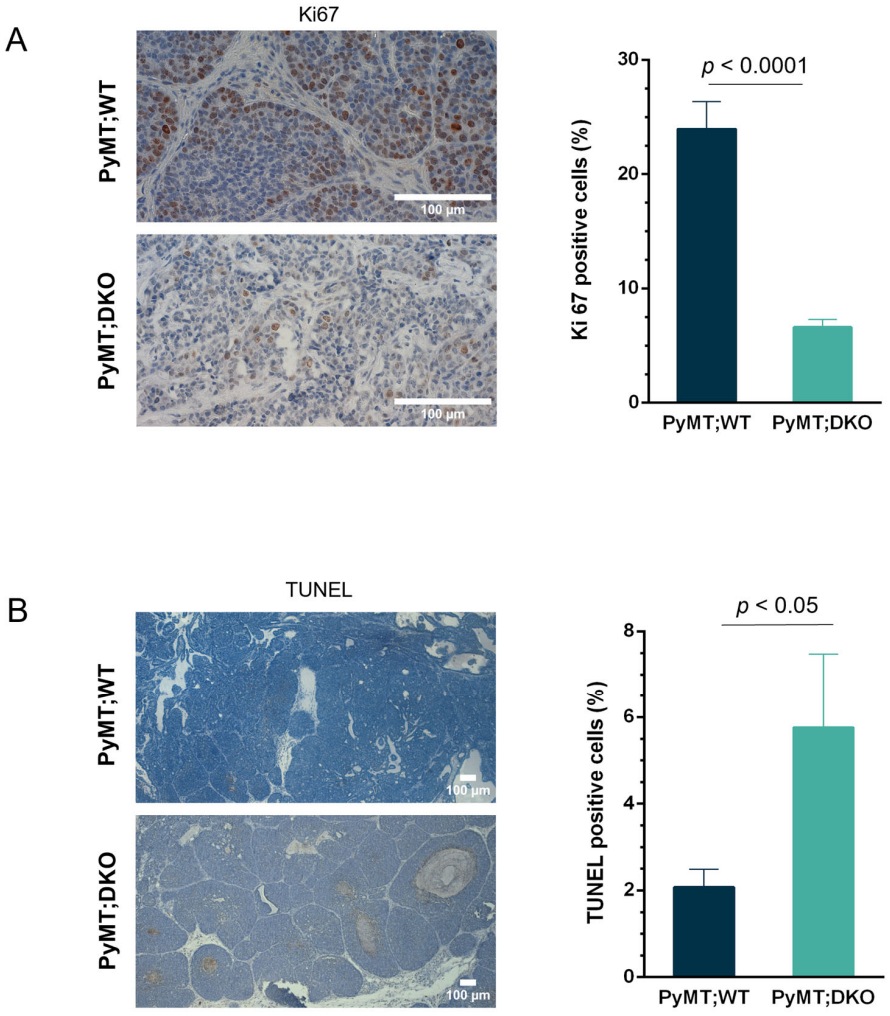

Figure 3. Effect of stefin B and cystatin C deficiency on proliferation and cell death. (**A**) Cell proliferation in primary tumors was determined through immunodetection of Ki67 in PyMT;WT and PyMT;DKO mice at 14 weeks of age. Representative images and quantification of Ki67-positive cells as a percentage of total cells in PyMT;WT (n = 11) and PyMT;DKO (n = 10) tumors. Ki67 index was calculated from 10 high-power fields per tumor using computer-assisted data analysis in ImageJ. Differences were analyzed using Student's *t*-test. (**B**) Cell death in primary tumors from PyMT;WT and PyMT;DKO mice at 14 weeks of age was determined through TUNEL assays. Representative images and quantification of TUNEL-positive cells as a percentage of total cells in PyMT;WT (n = 9) and PyMT;DKO (n = 8) tumors. The TUNEL+ index was calculated from 10 high-power fields per tumor using computer-assisted data analysis in ImageJ. Differences were analyzed using Student's *t*-test.

In addition to decreased tumor cell proliferation, tumor size may also decrease due to increased cell death or diminished tumor vascularization. Therefore, we assessed the extent of cancer cell apoptosis in primary PyMT tumors using terminal dUTP nick end labeling (TUNEL) staining, a technique that detects DNA fragmentation, a direct indicator of apoptosis. Notably, a significantly higher rate of apoptotic cell death in PyMT;DKO tumors was detected compared to PyMT;WT tumors (2.1% in the PyMT;WT group, 5.8% in the PyMT;DKO group) (Figure 3B).

We also examined the potential influence of CstC and StfB depletion on the vascularization of PyMT tumors by immunofluorescence staining of endothelial cells in primary tumor sections with a well-established marker of angiogenesis, CD31 (also known as platelet endothelial cell adhesion molecule-1 [PECAM-1]). The qualitative assessment and quantification of CD31 staining revealed no significant differences in average vessel density between PyMT;DKO and PyMT;WT tumors (Figure S3).

3.5. Effect of Stefin B and Cystatin C Deficiency on TAMs in the Tumor Microenvironment

Considering the integral role of macrophages in shaping the tumor microenvironment and influencing cancer progression, we evaluated whether CstC and StfB knockouts alter the presence of immune cells, specifically macrophages, within the tumor microenvironment. Tumor-associated macrophages (TAMs) modulate tumor growth, angiogenesis, and immune suppression, and their density and polarization state have been shown to greatly influence disease outcomes in many pre-clinical models, including the PyMT breast cancer model [56,57]. Macrophages were detected by immunohistochemical staining for F4/80, a well-established protein marker for murine macrophages. A higher presence of macrophages was observed in the PyMT;DKO tumors compared to the PyMT;WT group (Figure 4A,B). Additionally, staining for CD86, a marker of classically activated M1 macrophages, revealed a higher proportion of M1 macrophages in the PyMT;DKO tumor tissue (Figure 4C). Furthermore, we assessed M2 macrophage infiltration using CD206 immunohistochemistry but did not observe a statistically significant difference between the groups (Figure 4D). Taken together, the absence of CstC and StfB appears to have a substantial impact on the tumor microenvironment, promoting macrophage infiltration and a shift toward M1 macrophage polarization.

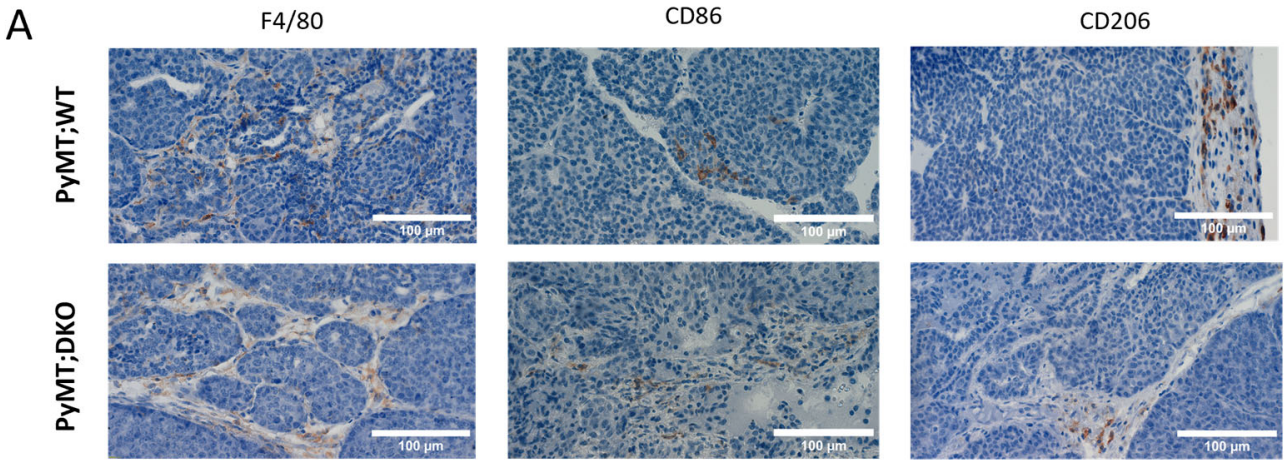

Figure 4. *Cont.*

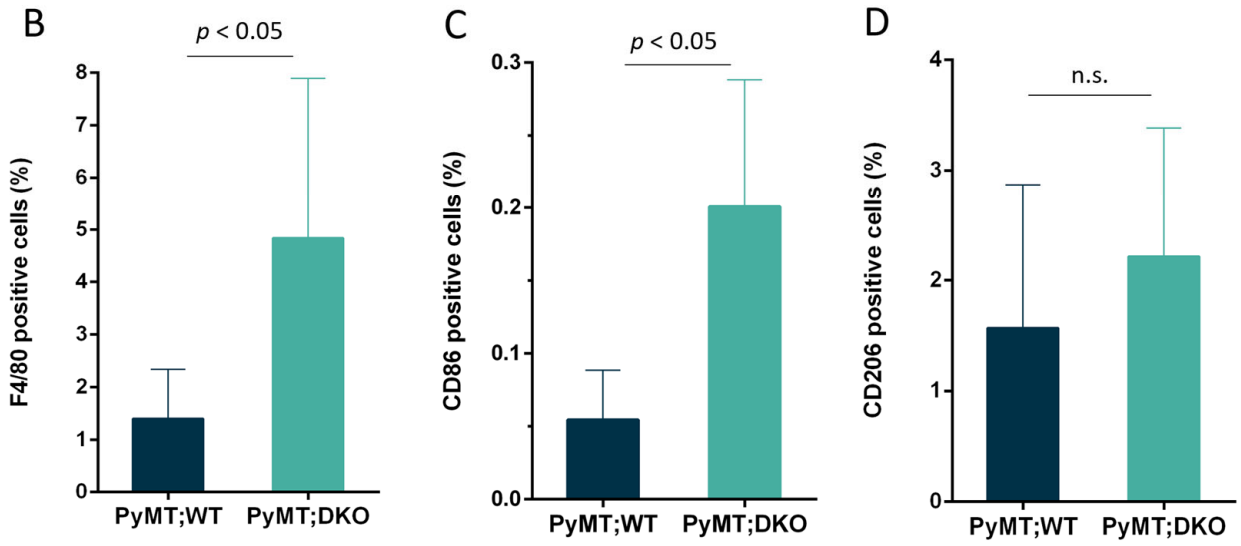

Figure 4. Effect of stefin B and cystatin C deficiency on macrophage infiltration and polarization in PyMT mammary tumors. (**A**) Representative images of immunohistochemical staining for F4/80 (macrophages), CD206 (M2 macrophages), and CD86 (M1 macrophages) in tumors from PyMT;WT and PyMT;DKO mice at 14 weeks of age. Scale bar: 100 µm. (**B**) Quantification of F4/80-positive cells as a percentage of total cells in PyMT;WT (n = 5) and PyMT;DKO (n = 5) tumors. (**C**) Quantification of CD86-positive cells, as a percentage of total cells in PyMT;WT (n = 5) and PyMT;DKO (n = 5) tumors. (**D**) Quantification of CD206-positive cells as a percentage of total cells in PyMT;WT (n = 6) and PyMT;DKO (n = 6) tumors. n.s., not significant. Statistical significance was assessed using Student's *t*-test.

4. Discussion

The precise regulation of proteolytic activity is necessary for maintaining cellular and organismal homeostasis, whereas unbalanced proteolysis can alter cellular metabolism and lead to the development of pathological processes, including cancer [58]. Improving our understanding of protease function and its regulation by inhibitors in complex processes that contribute to disease development and progression is crucial for developing more effective treatment strategies. Among the protease families, cysteine cathepsins constitute a major group of lysosomal proteases that are frequently upregulated and/or mislocalized in tumors. By altering basement membranes, breaking down extracellular matrix (ECM), and modifying pro-tumor signaling in the tumor microenvironment, they impact cancer progression [4,59]. In multiple cancer types, cathepsin activity is directly associated with invasion, angiogenesis, metastasis, and response to therapy, as shown by experimental and clinical data [59]. The inhibition of protease activity by endogenous protein inhibitors is a crucial regulatory mechanism for these enzymes. Therefore, we have researched the roles of stefin B and cystatin C, potent intracellular and extracellular inhibitors of cysteine cathepsins, respectively, which have been associated with numerous pathological conditions, including cancer [60]. Apart from inhibiting proteases, they can also exert protease-independent signaling effects that are important for tumor biology, such as regulating immune cell function and cell survival pathways [61,62].

In the field of cancer biology, the traditional view on protease–inhibitor interactions becomes considerably more complex, as these proteins engage in diverse signaling and immune modulatory functions. In this study, we used the PyMT transgenic mouse model, which replicates the progression of multistage breast cancer and spontaneously develops pulmonary metastases, to investigate the effects of stefin B and cystatin C deficiency on the development and metastasis of breast cancer. According to earlier studies, stefin B provides

cytoprotection against oxidative damage by preserving lysosomal membrane integrity and conferring FLIP (FLICE-like inhibitory protein)-mediated apoptotic resistance [35]. At the same time, cystatin C maintains growth-promoting signals by stabilizing 14-3-3 proteins and modulating the TGF-β pathway [48]. These diverse roles demonstrate how evolution has advanced from simple proteolytic regulation to complex cellular control systems [40]. The distinct subcellular localization of intracellular stefin B versus secreted cystatin C has enabled each inhibitor to develop specific functions that affect tumor biology through mechanisms other than independent direct protease inhibition.

Contrary to their expected tumor-suppressive functions, our findings show that stefin B and cystatin C act as tumor promoters in this murine model. Compared to single knockouts, a combined deficiency of both inhibitors resulted in impaired tumor development, characterized by a delayed tumor onset and reduced tumor growth. These results confirm that the roles of proteases and their inhibitors can vary depending on the tissue type, disease stage, subcellular location, and microenvironmental factors. Consistent with this context dependency, our findings align with clinical observations in human colorectal cancer patients, where elevated serum levels of stefin B and cystatin C have been associated with advanced disease stage and poorer survival outcomes [36]. This concordance between experimental and clinical data supports the concept that these inhibitors' functions could extend beyond canonical proteolytic regulation.

In this study, we investigated the combined depletion of stefin B and cystatin C in the PyMT mouse breast cancer model (PyMT;DKO), which is relevant to our previously published work on individual gene knockouts [35,48]. We have shown that the combined loss of stefin B and cystatin C resulted in significantly higher tumor suppression than either knockout alone. Specifically, PyMT;DKO tumors exhibited a 41% reduction in cumulative tumor weight compared to PyMT;WT controls (average tumor weight 5.8 g vs. 9.8 g in WT), substantially exceeding the 23% reduction observed with single knockout of stefin B (average tumor weight 6.47 g vs. 8.44 g in WT) [35] or 23% reduction with single knockout of cystatin C (average tumor weight 7.1 g vs. 9.2 g in WT) [48]. Taken together, this implies that tumor cells use multiple survival strategies and that, when these strategies are disrupted simultaneously, synergistic vulnerabilities arise that outweigh the consequences of focusing on a single pathway. This enhanced effect likely reflects the coordinated disruption of stefin B-mediated stress resistance [35] and cystatin C-mediated growth support [48], although the precise molecular mechanisms underlying this synergy in our model remain to be investigated. The superior tumor suppression observed in our double-knockout compared with single-gene deletions suggests that these inhibitors may function through complementary rather than redundant pathways.

The pronounced apoptosis detected in PyMT;DKO tumors indicates heightened susceptibility to cell death. The elevated apoptosis observed in PyMT;DKO tumors correlated with a higher frequency of islands of dead cells, aligning with histological findings in stefin B-deficient tumors [35]. The enhanced apoptosis likely results from multiple converging mechanisms. The literature suggests that stefin B loss permits cathepsin-mediated degradation of Bcl-2 family proteins and the activation of the intrinsic apoptotic pathway. At the same time, concurrent FLIP destabilization may sensitize cells to death receptor engagement. Mechanistically, previous studies indicate that this likely reflects oxidative stress-induced lysosomal destabilization, in which stefin B normally protects against inappropriate cathepsin release into the cytosol. Upon oxidative challenge, cathepsins leak into the cytoplasm and cleave pro-apoptotic Bcl-2 family members (Bid, Bcl-xL, Mcl-1), with Bid cleaved into tBid, thereby activating intrinsic apoptosis via caspases-3 and -7. Furthermore, it has been shown that stefin B has protease-independent cytoprotective effects, such as stabilizing FLIP, which inhibits death receptor signaling by competing with caspase-8 for

the binding of FADD [63]. Although a deficiency of cystatin C alone has been reported to be anti-apoptotic [48], our PyMT;DKO model shows that stefin B-associated effects are primarily responsible for the enhanced apoptosis. These findings support the concept that stefin B protects cancer cells from stress-induced death through pathways independent of cathepsin inhibition and that loss of these protective functions sensitizes tumor cells to apoptosis, most likely contributing to the reduced tumor growth we observed.

The ability of the PyMT model to induce spontaneous pulmonary metastases provides insight into mechanisms controlling tumor dissemination. In contrast to single-gene deletions, where stefin B loss results in no metastatic phenotype and cystatin C deficiency promotes dissemination [35,48], PyMT;DKO tumors displayed altered metastatic potential, with reduced numbers of lung metastases. These findings demonstrate that protease inhibitor expression affects not only tumor cell-intrinsic pathways but also processes critical for tumor cell dissemination. As metastasis is a multistep process influenced by multiple factors, including tumor cell survival in circulation, extravasation and colonization efficiency within the target organ microenvironment ("seed and soil" theory), immune surveillance, and other host-related factors, the reduced metastatic burden in the double-knockout suggests that the loss of cystatin C and stefin B synergistically reshapes the tumor microenvironment to further restrict metastatic dissemination, with reduced proliferation and increased apoptosis rate of PyMT;DKO tumor cells potentially contributing to this mechanism.

By promoting angiogenesis, immune evasion, and therapy resistance, the tumor microenvironment (TME) plays a pivotal role in shaping cancer progression [64]. It represents a dynamic and complex ecosystem composed of cancer cells, stromal cells, immune cells, blood vessels, extracellular matrix, and various signaling molecules that interact dynamically to support tumor growth, survival, and metastasis [65,66]. Among the immune cells infiltrating the TME, tumor-associated macrophages (TAMs) are critical components that can significantly influence cancer progression [67]. In our study, we demonstrated a substantial increase in F4/80-positive macrophages in PyMT;DKO tumors. Furthermore, our analysis demonstrated a reprogramming of the TME toward a tumor-suppressive state, as evidenced by an increase in CD86-positive M1 macrophages without a corresponding expansion of CD206-positive M2 populations. M1-polarized macrophages exert anti-tumor functions through inflammatory mediator production, reactive species generation, and direct cytolytic activity [68,69]. Although the underlying mechanisms remain to be fully elucidated, this macrophage reprogramming may be linked to the loss of cystatin C, which has been shown to modulate macrophage cytokine profiles and inflammatory responses, including regulation of TNF-α and IL-10 production [51]. Our observation of increased M1 macrophage infiltration aligns with recent findings from a syngeneic pancreatic cancer model, in which CRISPR-mediated cystatin C knockout similarly reduced tumor growth and remodeled the tumor immune microenvironment by diminishing recruitment of immunosuppressive TREM2+ macrophages [50]. Although Kleeman et al. demonstrated reduced protumorigenic macrophage populations, the PyMT;DKO model showed increased M1 populations, yet both mechanisms result in remodeling of the tumor microenvironment toward an anti-tumor state. The M1 shift we observed may therefore represent a specific disruption of tumor-associated immunosuppressive mechanisms, which would likely support the observed tumor growth reduction and contribute to the multilayered tumor suppression in the PyMT;DKO model. This shift in macrophage polarization toward M1 contrasts with typical tumor-associated macrophage profiles, in which M2-polarized macrophages usually predominate and promote tumor progression through immunosuppressive functions, angiogenesis, and tissue remodeling [70,71]. The simultaneous loss of stefin B and cystatin C appears to alter signaling networks that normally recruit and

polarize macrophages toward pro-tumorigenic phenotypes, creating conditions particularly hostile to the survival and proliferation of tumor cells.

5. Conclusions

Overall, our study demonstrates that stefin B and cystatin C function as tumor promoters in breast cancer through modulation of tumor metabolism, and that their combined loss enhances tumor suppression. The superior anti-tumor effects we observed indicate that these inhibitors most likely act through complementary mechanisms that support tumor growth, although the precise molecular pathways warrant further investigation. Simultaneous ablation of both inhibitors revealed therapeutic vulnerabilities inaccessible with single-target approaches, suggesting potential benefits of dual-targeting strategies. Notably, an observed increase in intratumoral M1 macrophage populations may contribute to the disruption of tumor-associated immunosuppressive mechanisms, thus affecting tumor cell survival and proliferation leading to reduced tumor volume and metastasis in PyMT mice lacking both inhibitor genes. Our findings are hypothesis-generating and provide a foundation for future research aimed at understanding the molecular basis of the synergistic effects we observed, determining the therapeutic potential of combined inhibitor targeting across different cancer models, and exploring integration with existing therapeutic approaches. This study challenges traditional views of protease inhibitor functions in cancer and emphasizes the importance of exploring their roles in tumor biology, including their impact on tumor metabolic pathways, and the potential to redefine current therapeutic strategies.

Supplementary Materials: The following supporting information can be downloaded at: https://www.mdpi.com/article/10.3390/cells15040360/s1, Figure S1: Comparative histological assessment of tissues from mice with different genotypes. Hematoxylin and eosin staining of liver, kidney, lung, and spleen from PyMT;WT, PyMT;DKO, PyMT;*StfB*$^{-/-}$ and PyMT;*CstC*$^{-/-}$ mice. Organs were collected, dehydrated, embedded in paraffin, sectioned at 5 µm, and stained with hematoxylin and eosin. A pathohistological examination of the organs was performed. Scale bar: 100 µm. Figure S2: Cell proliferation of PyMT;WT (n = 6) and PyMT;DKO (n = 6) primary tumor cells determined by BrdU incorporation assay. Cell proliferation was assessed by BrdU cell proliferation assay HTS kit. PyMT;WT and PyMT;DKO cells were cultured and treated as described in the assay kit. Figure S3: Immunofluorescence analysis of CD31 expression in PyMT;WT and PyMT;DKO mammary tumors. (A) Representative images of immunofluorescence staining of the endothelial cell-specific marker CD31 (red staining) on PyMT;WT and PyMT;DKO tumors. Scale bar: 100µM. (B) Quantification of CD31 positive area as percentage of all tumor area in PyMT;WT (n = 8) and PyMT;DKO (n = 9) tumors. Statistics were analyzed using Student's *t*-test. Figure S4: Original Western blot images and densitometric analysis for Figure 1A. (A) Original membrane probed for stefin B. (B) Original membrane probed for β-actin (loading control). (C) Bar graph showing densitometric quantification of stefin B expression normalized to β-actin. Bars represent mean values ± standard deviation (SD). Densitometric analysis was performed using ImageJ software. Statistical significance was determined using Student's *t*-test. Figure S5: Original Western blot images and densitometric analysis for Figure 1B. (A) Original membrane probed for cystatin C. (B) Original membrane probed for β-actin (loading control). (**C**) Bar graph showing densitometric quantification of cystatin C expression normalized to β-actin. Bars represent mean values ± standard deviation (SD). Densitometric analysis was performed using ImageJ software. Statistical significance was determined using Student's *t*-test.

Author Contributions: Conceptualization, O.V.; methodology, O.V., J.Z., M.B. and G.M.; formal analysis, P.M.Š. and J.Z.; writing—original draft preparation, P.M.Š.; writing—review and editing, O.V. and G.M.; visualization, P.M.Š.; supervision, B.T., G.M. and O.V.; project administration, O.V.; funding acquisition, O.V. and B.T. All authors have read and agreed to the published version of the manuscript.

Funding: This research was funded by the Slovenian Research and Innovation Agency (grant number P1-0140).

Institutional Review Board Statement: The animal study protocol was approved by the Ethics Committee of Administration of the Republic of Slovenia for food safety, veterinary, and plant protection (ethical approval codes: U34401-35/2014/2, date of approval: 6 October 2014; U34401-6/2019/5, date of approval: 14 March 2019; and U34401-5/2022/15, date of approval: 30 June 2022). Procedures for animal care and experiments were in accordance with the "Guide for the Care and Use in Laboratory Animals".

Informed Consent Statement: Not applicable.

Data Availability Statement: The original contributions presented in this study are included in the article/Supplementary Materials. Further inquiries can be directed to the corresponding author.

Acknowledgments: We thank Ivica Štefe for her technical support and Andreja Kozak and Ernestina Lavrih for their valuable discussions. We acknowledge Servier Medical Art for providing the macrophage and mouse-gray icons used in the graphical abstract (https://smart.servier.com/, accessed on 15 December 2025), licensed under CC-BY 3.0 Unported (https://creativecommons.org/licenses/by/3.0/, accessed on 15 December 2025). The icons' colors were modified for the graphical design.

Conflicts of Interest: Author Olga Vasiljeva was employed by the company CytomX Therapeutics. The remaining authors declare that the research was conducted in the absence of any commercial or financial relationships that could be construed as a potential conflict of interest.

Abbreviations

The following abbreviations are used in this manuscript:

AMPK	AMP-activated protein kinase
BrdU	5-bromo-2′-deoxyuridine
CstC	Cystatin C
DAB	3,3′-Diaminobenzidine
DKO	Double-knockout
DMEM	Dulbecco's Modified Eagle Medium
DNA	Deoxyribonucleic acid
DTT	Dithiothreitol
ECM	Extracellular matrix
EDTA	Ethylenediaminetetraacetic acid
EMT	Epithelial–mesenchymal transition
FADD	Fas-associated death domain
FBS	Fetal bovine serum
FLIP	FLICE-like inhibitory protein
IHC	Immunohistochemistry
MAPK	Mitogen-activated protein kinase
MMTV	Mouse mammary tumor virus
mTOR	Mechanistic target of rapamycin
PBS	Phosphate-buffered saline
PECAM-1	Platelet endothelial cell adhesion molecule-1
PI3K	Phosphoinositide 3-kinase
PyMT	Polyoma Middle T antigen
RIPA	Radioimmunoprecipitation assay
ROS	Reactive oxygen species
SDS-PAGE	Sodium dodecyl sulfate-polyacrylamide gel electrophoresis
StfB	Stefin B
TAMs	Tumor-associated macrophages
TGF-β	Transforming growth factor beta
TME	Tumor microenvironment

TNF-α	Tumor necrosis factor alpha
TREM2	Triggering receptor expressed on myeloid cells 2
TUNEL	Terminal deoxynucleotidyl transferase dUTP nick end labeling
WT	Wild-type
Z-Phe-Arg-AMC	Z-Phenylalanyl-arginyl-7-amido-4-methylcoumarin

References

1. Turk, V.; Stoka, V.; Vasiljeva, O.; Renko, M.; Sun, T.; Turk, B.; Turk, D. Cysteine cathepsins: From structure, function and regulation to new frontiers. *Biochim. Biophys. Acta* **2012**, *1824*, 68–88. [CrossRef]
2. Vidak, E.; Javoršek, U.; Vizovišek, M.; Turk, B. Cysteine Cathepsins and their Extracellular Roles: Shaping the Microenvironment. *Cells* **2019**, *8*, 264. [CrossRef] [PubMed]
3. Yadati, T.; Houben, T.; Bitorina, A.; Shiri-Sverdlov, R. The Ins and Outs of Cathepsins: Physiological Function and Role in Disease Management. *Cells* **2020**, *9*, 1679. [CrossRef] [PubMed]
4. Mohamed, M.M.; Sloane, B.F. Multifunctional enzymes in cancer. *Nat. Rev. Cancer* **2006**, *6*, 764–775. [CrossRef] [PubMed]
5. Reiser, J.; Adair, B.; Reinheckel, T. Specialized roles for cysteine cathepsins in health and disease. *J. Clin. Investig.* **2010**, *120*, 3421–3431. [CrossRef]
6. Drake, M.T.; Clarke, B.L.; Oursler, M.J.; Khosla, S. Cathepsin K Inhibitors for Osteoporosis: Biology, Potential Clinical Utility, and Lessons Learned. *Endocr. Rev.* **2017**, *38*, 325–350. [CrossRef]
7. Li, Q.; Zhou, Z.; Xu, T.; Gao, X.; Lou, Y.; Chen, Z.; Zhang, M.; Fang, Q.; Tan, J.; Huang, J. Relationship between cathepsins and cardiovascular diseases: A Mendelian randomized study. *Front. Pharmacol.* **2024**, *15*, 1370350. [CrossRef]
8. Vasiljeva, O.; Reinheckel, T.; Peters, C.; Turk, D.; Turk, V.; Turk, B. Emerging roles of cysteine cathepsins in disease and their potential as drug targets. *Curr. Pharm. Des.* **2007**, *13*, 387–403. [CrossRef]
9. Vizin, T.; Christensen, I.J.; Nielsen, H.J.; Kos, J. Cathepsin X in serum from patients with colorectal cancer: Relation to prognosis. *Radiol. Oncol.* **2012**, *46*, 207–212. [CrossRef]
10. Duong, L.T.; Wesolowski, G.A.; Leung, P.; Oballa, R.; Pickarski, M. Efficacy of a cathepsin K inhibitor in a preclinical model for prevention and treatment of breast cancer bone metastasis. *Mol. Cancer Ther.* **2014**, *13*, 2898–2909. [CrossRef]
11. Bian, B.; Mongrain, S.; Cagnol, S.; Langlois, M.J.; Boulanger, J.; Bernatchez, G.; Carrier, J.C.; Boudreau, F.; Rivard, N. Cathepsin B promotes colorectal tumorigenesis, cell invasion, and metastasis. *Mol. Carcinog.* **2016**, *55*, 671–687. [CrossRef] [PubMed]
12. Olson, O.C.; Joyce, J.A. Cysteine cathepsin proteases: Regulators of cancer progression and therapeutic response. *Nat. Rev. Cancer* **2015**, *15*, 712–729. [CrossRef] [PubMed]
13. Liu, W.L.; Liu, D.; Cheng, K.; Liu, Y.J.; Xing, S.; Chi, P.D.; Liu, X.H.; Xue, N.; Lai, Y.Z.; Guo, L.; et al. Evaluating the diagnostic and prognostic value of circulating cathepsin S in gastric cancer. *Oncotarget* **2016**, *7*, 28124–28138. [CrossRef] [PubMed]
14. Greten, F.R.; Grivennikov, S.I. Inflammation and Cancer: Triggers, Mechanisms, and Consequences. *Immunity* **2019**, *51*, 27–41. [CrossRef]
15. Stoka, V.; Vasiljeva, O.; Nakanishi, H.; Turk, V. The Role of Cysteine Protease Cathepsins B, H, C, and X/Z in Neurodegenerative Diseases and Cancer. *Int. J. Mol. Sci.* **2023**, *24*, 15613. [CrossRef]
16. Jakoš, T.; Pišlar, A.; Jewett, A.; Kos, J. Cysteine Cathepsins in Tumor-Associated Immune Cells. *Front. Immunol.* **2019**, *10*, 2037. [CrossRef]
17. Zhang, G.P.; Yue, X.; Li, S.Q. Cathepsin C Interacts with TNF-α/p38 MAPK Signaling Pathway to Promote Proliferation and Metastasis in Hepatocellular Carcinoma. *Cancer Res. Treat.* **2020**, *52*, 10–23. [CrossRef]
18. Gogineni, V.R.; Gupta, R.; Nalla, A.K.; Velpula, K.K.; Rao, J.S. uPAR and cathepsin B shRNA impedes TGF-β1-driven proliferation and invasion of meningioma cells in a XIAP-dependent pathway. *Cell Death Dis.* **2012**, *3*, e439. [CrossRef]
19. Tummalapalli, P.; Spomar, D.; Gondi, C.S.; Olivero, W.C.; Gujrati, M.; Dinh, D.H.; Rao, J.S. RNAi-mediated abrogation of cathepsin B and MMP-9 gene expression in a malignant meningioma cell line leads to decreased tumor growth, invasion and angiogenesis. *Int. J. Oncol.* **2007**, *31*, 1039–1050. [CrossRef]
20. Overall, C.M.; Dean, R.A. Degradomics: Systems biology of the protease web. Pleiotropic roles of MMPs in cancer. *Cancer Metastasis Rev.* **2006**, *25*, 69–75. [CrossRef]
21. Vasiljeva, O.; Turk, B. Dual contrasting roles of cysteine cathepsins in cancer progression: Apoptosis versus tumour invasion. *Biochimie* **2008**, *90*, 380–386. [CrossRef]
22. Turk, B.; Turk, D.; Turk, V. Protease signalling: The cutting edge. *Embo J.* **2012**, *31*, 1630–1643. [CrossRef] [PubMed]
23. Žerovnik, E. Human stefin B: From its structure, folding, and aggregation to its function in health and disease. *Front. Mol. Neurosci.* **2022**, *15*, 1009976. [CrossRef] [PubMed]
24. Breznik, B.; Mitrović, A.; Lah, T.T.; Kos, J. Cystatins in cancer progression: More than just cathepsin inhibitors. *Biochimie* **2019**, *166*, 233–250. [CrossRef] [PubMed]
25. Kopitar-Jerala, N. The Role of Stefin B in Neuro-inflammation. *Front. Cell. Neurosci.* **2015**, *9*, 458. [CrossRef]

26. Trstenjak-Prebanda, M.; Biasizzo, M.; Dolinar, K.; Pirkmajer, S.; Turk, B.; Brault, V.; Herault, Y.; Kopitar-Jerala, N. Stefin B Inhibits NLRP3 Inflammasome Activation via AMPK/mTOR Signalling. *Cells* **2023**, *12*, 2731. [CrossRef]
27. Pogorzelska, A.; Żołnowska, B.; Bartoszewski, R. Cysteine cathepsins as a prospective target for anticancer therapies—Current progress and prospects. *Biochimie* **2018**, *151*, 85–106. [CrossRef]
28. Wang, X.; Gui, L.; Zhang, Y.; Zhang, J.; Shi, J.; Xu, G. Cystatin B is a progression marker of human epithelial ovarian tumors mediated by the TGF-β signaling pathway. *Int. J. Oncol.* **2014**, *44*, 1099–1106. [CrossRef]
29. Tamhane, T.; Lllukkumbura, R.; Lu, S.; Maelandsmo, G.M.; Haugen, M.H.; Brix, K. Nuclear cathepsin L activity is required for cell cycle progression of colorectal carcinoma cells. *Biochimie* **2016**, *122*, 208–218. [CrossRef]
30. Strojan, P.; Budihna, M.; Smid, L.; Svetic, B.; Vrhovec, I.; Kos, J.; Skrk, J. Prognostic significance of cysteine proteinases cathepsins B and L and their endogenous inhibitors stefins A and B in patients with squamous cell carcinoma of the head and neck. *Clin. Cancer Res.* **2000**, *6*, 1052–1062.
31. Lin, Y.Y.; Chen, Z.W.; Lin, Z.P.; Lin, L.B.; Yang, X.M.; Xu, L.Y.; Xie, Q. Tissue Levels of Stefin A and Stefin B in Hepatocellular Carcinoma. *Anat. Rec.* **2016**, *299*, 428–438. [CrossRef] [PubMed]
32. Levicar, N.; Kos, J.; Blejec, A.; Golouh, R.; Vrhovec, I.; Frkovic-Grazio, S.; Lah, T.T. Comparison of potential biological markers cathepsin B, cathepsin L, stefin A and stefin B with urokinase and plasminogen activator inhibitor-1 and clinicopathological data of breast carcinoma patients. *Cancer Detect. Prev.* **2002**, *26*, 42–49. [CrossRef] [PubMed]
33. Gole, B.; Huszthy, P.C.; Popović, M.; Jeruc, J.; Ardebili, Y.S.; Bjerkvig, R.; Lah, T.T. The regulation of cysteine cathepsins and cystatins in human gliomas. *Int. J. Cancer* **2012**, *131*, 1779–1789. [CrossRef] [PubMed]
34. Feldman, A.S.; Banyard, J.; Wu, C.L.; McDougal, W.S.; Zetter, B.R. Cystatin B as a tissue and urinary biomarker of bladder cancer recurrence and disease progression. *Clin. Cancer Res.* **2009**, *15*, 1024–1031. [CrossRef]
35. Butinar, M.; Prebanda, M.T.; Rajković, J.; Jerič, B.; Stoka, V.; Peters, C.; Reinheckel, T.; Krüger, A.; Turk, V.; Turk, B.; et al. Stefin B deficiency reduces tumor growth via sensitization of tumor cells to oxidative stress in a breast cancer model. *Oncogene* **2014**, *33*, 3392–3400. [CrossRef]
36. Kos, J.; Krašovec, M.; Cimerman, N.; Nielsen, H.J.; Christensen, I.J.; Brünner, N. Cysteine Proteinase Inhibitors Stefin A, Stefin B, and Cystatin C in Sera from Patients with Colorectal Cancer: Relation to Prognosis. *Clin. Cancer Res.* **2000**, *6*, 505–511.
37. Shiraishi, T.; Mori, M.; Tanaka, S.; Sugimachi, K.; Akiyoshi, T. Identification of cystatin B in human esophageal carcinoma, using differential displays in which the gene expression is related to lymph-node metastasis. *Int. J. Cancer* **1998**, *79*, 175–178. [CrossRef]
38. McDonald, S.L.; Edington, H.D.; Kirkwood, J.M.; Becker, D. Expression analysis of genes identified by molecular profiling of VGP melanomas and MGP melanoma-positive lymph nodes. *Cancer Biol. Ther.* **2004**, *3*, 110–120. [CrossRef]
39. Rawlings, N.D.; Barrett, A.J.; Thomas, P.D.; Huang, X.; Bateman, A.; Finn, R.D. The MEROPS database of proteolytic enzymes, their substrates and inhibitors in 2017 and a comparison with peptidases in the PANTHER database. *Nucleic Acids Res.* **2018**, *46*, D624–D632. [CrossRef]
40. Leto, G.; Crescimanno, M.; Flandina, C. On the role of cystatin C in cancer progression. *Life Sci.* **2018**, *202*, 152–160. [CrossRef]
41. Sheikh, A.M.; Wada, Y.; Tabassum, S.; Inagaki, S.; Mitaki, S.; Yano, S.; Nagai, A. Aggregation of Cystatin C Changes Its Inhibitory Functions on Protease Activities and Amyloid β Fibril Formation. *Int. J. Mol. Sci.* **2021**, *22*, 9682. [CrossRef] [PubMed]
42. Stańczykiewicz, B.; Łuc, M.; Banach, M.; Zabłocka, A. Cystatins: Unravelling the biological implications for neuroprotection. *Arch. Med. Sci.* **2024**, *20*, 157–166. [CrossRef] [PubMed]
43. Fernando, S.; Polkinghorne, K.R. Cystatin C: Not just a marker of kidney function. *Braz. J. Nephrol.* **2020**, *42*, 6–7. [CrossRef] [PubMed]
44. Keppler, D. Towards novel anti-cancer strategies based on cystatin function. *Cancer Lett.* **2006**, *235*, 159–176. [CrossRef]
45. Xu, Y.; Ding, Y.; Li, X.; Wu, X. Cystatin C is a disease-associated protein subject to multiple regulation. *Immunol. Cell Biol.* **2015**, *93*, 442–451. [CrossRef]
46. Magister, S.; Kos, J. Cystatins in immune system. *J. Cancer* **2013**, *4*, 45–56. [CrossRef]
47. Cox, J.L. Cystatins and cancer. *Front. Biosci.* **2009**, *14*, 463–474. [CrossRef]
48. Završnik, J.; Butinar, M.; Prebanda, M.T.; Krajnc, A.; Vidmar, R.; Fonović, M.; Grubb, A.; Turk, V.; Turk, B.; Vasiljeva, O. Cystatin C deficiency suppresses tumor growth in a breast cancer model through decreased proliferation of tumor cells. *Oncotarget* **2017**, *8*, 73793–73809. [CrossRef]
49. Konduri, S.D.; Yanamandra, N.; Siddique, K.; Joseph, A.; Dinh, D.H.; Olivero, W.C.; Gujrati, M.; Kouraklis, G.; Swaroop, A.; Kyritsis, A.P.; et al. Modulation of cystatin C expression impairs the invasive and tumorigenic potential of human glioblastoma cells. *Oncogene* **2002**, *21*, 8705–8712. [CrossRef]
50. Kleeman, S.O.; Thakir, T.M.; Demestichas, B.; Mourikis, N.; Loiero, D.; Ferrer, M.; Bankier, S.; Riazat-Kesh, Y.; Lee, H.; Chantzichristos, D.; et al. Cystatin C is glucocorticoid responsive, directs recruitment of Trem2+ macrophages, and predicts failure of cancer immunotherapy. *Cell Genom.* **2023**, *3*, 100347. [CrossRef]
51. Frendéus, K.H.; Wallin, H.; Janciauskiene, S.; Abrahamson, M. Macrophage responses to interferon-γ are dependent on cystatin C levels. *Int. J. Biochem. Cell Biol.* **2009**, *41*, 2262–2269. [CrossRef]

52. Vasiljeva, O.; Korovin, M.; Gajda, M.; Brodoefel, H.; Bojic, L.; Krüger, A.; Schurigt, U.; Sevenich, L.; Turk, B.; Peters, C.; et al. Reduced tumour cell proliferation and delayed development of high-grade mammary carcinomas in cathepsin B-deficient mice. *Oncogene* **2008**, *27*, 4191–4199. [CrossRef]
53. Vasiljeva, O.; Papazoglou, A.; Krüger, A.; Brodoefel, H.; Korovin, M.; Deussing, J.; Augustin, N.; Nielsen, B.S.; Almholt, K.; Bogyo, M.; et al. Tumor cell-derived and macrophage-derived cathepsin B promotes progression and lung metastasis of mammary cancer. *Cancer Res.* **2006**, *66*, 5242–5250. [CrossRef] [PubMed]
54. Guy, C.T.; Cardiff, R.D.; Muller, W.J. Induction of mammary tumors by expression of polyomavirus middle T oncogene: A transgenic mouse model for metastatic disease. *Mol. Cell. Biol.* **1992**, *12*, 954–961. [CrossRef] [PubMed]
55. Lin, E.Y.; Jones, J.G.; Li, P.; Zhu, L.; Whitney, K.D.; Muller, W.J.; Pollard, J.W. Progression to malignancy in the polyoma middle T oncoprotein mouse breast cancer model provides a reliable model for human diseases. *Am. J. Pathol.* **2003**, *163*, 2113–2126. [CrossRef] [PubMed]
56. Qian, B.Z.; Pollard, J.W. Macrophage diversity enhances tumor progression and metastasis. *Cell* **2010**, *141*, 39–51. [CrossRef]
57. Lin, E.Y.; Nguyen, A.V.; Russell, R.G.; Pollard, J.W. Colony-stimulating factor 1 promotes progression of mammary tumors to malignancy. *J. Exp. Med.* **2001**, *193*, 727–740. [CrossRef]
58. Turk, B.; Turk, D.; Salvesen, G.S. Regulating cysteine protease activity: Essential role of protease inhibitors as guardians and regulators. *Curr. Pharm. Des.* **2002**, *8*, 1623–1637. [CrossRef]
59. Gocheva, V.; Zeng, W.; Ke, D.; Klimstra, D.; Reinheckel, T.; Peters, C.; Hanahan, D.; Joyce, J.A. Distinct roles for cysteine cathepsin genes in multistage tumorigenesis. *Genes Dev.* **2006**, *20*, 543–556. [CrossRef]
60. Turk, V.; Stoka, V.; Turk, D. Cystatins: Biochemical and structural properties, and medical relevance. *Front. Biosci.* **2008**, *13*, 5406–5420. [CrossRef]
61. Polajnar, M.; Zavašnik-Bergant, T.; Škerget, K.; Vizovišek, M.; Vidmar, R.; Fonović, M.; Kopitar-Jerala, N.; Petrovič, U.; Navarro, S.; Ventura, S.; et al. Human stefin B role in cell's response to misfolded proteins and autophagy. *PLoS ONE* **2014**, *9*, e102500. [CrossRef] [PubMed]
62. Polajnar, M.; Ceru, S.; Kopitar-Jerala, N.; Zerovnik, E. Human stefin B normal and patho-physiological role: Molecular and cellular aspects of amyloid-type aggregation of certain EPM1 mutants. *Front. Mol. Neurosci.* **2012**, *5*, 88. [CrossRef] [PubMed]
63. Yang, F.; Tay, K.H.; Dong, L.; Thorne, R.F.; Jiang, C.C.; Yang, E.; Tseng, H.Y.; Liu, H.; Christopherson, R.; Hersey, P.; et al. Cystatin B inhibition of TRAIL-induced apoptosis is associated with the protection of $FLIP_L$ from degradation by the E3 ligase itch in human melanoma cells. *Cell Death Differ.* **2010**, *17*, 1354–1367. [CrossRef] [PubMed]
64. Gajewski, T.F.; Schreiber, H.; Fu, Y.-X. Innate and adaptive immune cells in the tumor microenvironment. *Nat. Immunol.* **2013**, *14*, 1014–1022. [CrossRef]
65. Balkwill, F.R.; Capasso, M.; Hagemann, T. The tumor microenvironment at a glance. *J. Cell Sci.* **2012**, *125*, 5591–5596. [CrossRef]
66. Hanahan, D.; Weinberg, R.A. Hallmarks of cancer: The next generation. *Cell* **2011**, *144*, 646–674. [CrossRef]
67. Bied, M.; Ho, W.W.; Ginhoux, F.; Blériot, C. Roles of macrophages in tumor development: A spatiotemporal perspective. *Cell. Mol. Immunol.* **2023**, *20*, 983–992. [CrossRef]
68. Chen, S.; Saeed, A.F.U.H.; Liu, Q.; Jiang, Q.; Xu, H.; Xiao, G.G.; Rao, L.; Duo, Y. Macrophages in immunoregulation and therapeutics. *Signal Transduct. Target. Ther.* **2023**, *8*, 207. [CrossRef]
69. Hallam, S.; Escorcio-Correia, M.; Soper, R.; Schultheiss, A.; Hagemann, T. Activated macrophages in the tumour microenvironment—Dancing to the tune of TLR and NF-κB. *J. Pathol.* **2009**, *219*, 143–152. [CrossRef]
70. Barbay, V.; Houssari, M.; Mekki, M.; Banquet, S.; Edwards-Lévy, F.; Henry, J.P.; Dumesnil, A.; Adriouch, S.; Thuillez, C.; Richard, V.; et al. Role of M2-like macrophage recruitment during angiogenic growth factor therapy. *Angiogenesis* **2015**, *18*, 191–200. [CrossRef]
71. Huang, R.; Kang, T.; Chen, S. The role of tumor-associated macrophages in tumor immune evasion. *J. Cancer Res. Clin. Oncol.* **2024**, *150*, 238. [CrossRef]

Disclaimer/Publisher's Note: The statements, opinions and data contained in all publications are solely those of the individual author(s) and contributor(s) and not of MDPI and/or the editor(s). MDPI and/or the editor(s) disclaim responsibility for any injury to people or property resulting from any ideas, methods, instructions or products referred to in the content.